Atmos. Meas. Tech., 7, 2907–2918, 2014
www.atmos-meas-tech.net/7/2907/2014/
doi:10.5194/amt-7-2907-2014

Atmospheric Measurement Techniques
Open Access

Derivation of tropospheric methane from TCCON CH_4 and HF total column observations

K. M. Saad[1], D. Wunch[1], G. C. Toon[1,2], P. Bernath[3], C. Boone[4], B. Connor[5], N. M. Deutscher[6,7], D. W. T. Griffith[6], R. Kivi[8], J. Notholt[7], C. Roehl[1], M. Schneider[9], V. Sherlock[10], and P. O. Wennberg[1]

[1]California Institute of Technology, Pasadena, CA, USA
[2]Jet Propulsion Laboratory, California Institute of Technology, Pasadena, CA, USA
[3]Old Dominion University, Norfolk, VA, USA
[4]University of Waterloo, Waterloo, Ontario, Canada
[5]BC Consulting, Ltd., Alexandra, New Zealand
[6]University of Wollongong, Wollongong, Australia
[7]University of Bremen, Bremen, Germany
[8]Finnish Meteorological Institute, Sodankylä, Finland
[9]Karlsruhe Institute of Technology, Karlsruhe, Germany
[10]National Institute of Water and Atmospheric Research, Wellington, New Zealand

Correspondence to: K. M. Saad (katsaad@caltech.edu)

Received: 15 February 2014 – Published in Atmos. Meas. Tech. Discuss.: 7 April 2014
Revised: 18 July 2014 – Accepted: 6 August 2014 – Published: 10 September 2014

Abstract. The Total Carbon Column Observing Network (TCCON) is a global ground-based network of Fourier transform spectrometers that produce precise measurements of column-averaged dry-air mole fractions of atmospheric methane (CH_4). Temporal variability in the total column of CH_4 due to stratospheric dynamics obscures fluctuations and trends driven by tropospheric transport and local surface fluxes that are critical for understanding CH_4 sources and sinks. We reduce the contribution of stratospheric variability from the total column average by subtracting an estimate of the stratospheric CH_4 derived from simultaneous measurements of hydrogen fluoride (HF). HF provides a proxy for stratospheric CH_4 because it is strongly correlated to CH_4 in the stratosphere, has an accurately known tropospheric abundance (of zero), and is measured at most TCCON stations. The stratospheric partial column of CH_4 is calculated as a function of the zonal and annual trends in the relationship between CH_4 and HF in the stratosphere, which we determine from ACE-FTS satellite data. We also explicitly take into account the CH_4 column averaging kernel to estimate the contribution of stratospheric CH_4 to the total column. The resulting tropospheric CH_4 columns are consistent with in situ aircraft measurements and augment existing observations in the troposphere.

1 Introduction

The most abundant hydrocarbon in the atmosphere, methane (CH_4) is a driver of background tropospheric chemistry and a significant radiative forcing gas. However, the long-term trends of atmospheric mixing ratios and fluctuations in the annual growth rate remain unexplained due to an incomplete understanding of its sources and sinks.

Analyses of temporal and geospatial trends of CH_4 require precise, continuous measurements with adequate spatial coverage. Several such monitoring networks, such as World Meteorological Organization (WMO) Global Atmospheric Watch and National Oceanic and Atmospheric Administration (NOAA) Global Monitoring Division, have measured methane for decades. These sites are often in locations primarily intended for background observations, and measurements are confined to the surface, primarily within the boundary layer. The Total Carbon Column Observing Network (TCCON), a ground-based network of near-infrared (NIR) Fourier transform spectrometers (FTS), measures dry-air mole fractions (DMFs) of several atmospheric trace gases, including CH_4, integrated over the entire atmospheric column. The column measurements are sensitive to the free troposphere in addition to the surface, which can allow for

better separation of transport from local emissions. Additionally, total column measurements are less sensitive to vertical transport and mixing, and thus meridional or zonal gradients in column measurements can be used to characterize regional-scale fluxes (Yang et al., 2007; Wunch et al., 2011a; Keppel-Aleks et al., 2011). Several TCCON stations are near in situ sites that provide surface, tall tower, and aircraft measurements, which we use to compare the final tropospheric column-averaged CH_4 DMFs.

Tropospheric trends of CH_4 are obscured in total column measurements by variability originating in the stratosphere, especially by vertical shifts of the tropopause. Several methods for accounting for stratospheric variability have been proposed, including incorporating the compact relationship between CH_4 and another chemical tracer in the stratosphere (e.g., Washenfelder et al., 2003; Payne et al., 2009; Angelbratt et al., 2011; Sepúlveda et al., 2012, 2014; Wang et al., 2014). Washenfelder et al. (2003) estimate the contribution of variations in stratospheric CH_4 as the product of the hydrogen fluoride (HF) column-averaged DMF and the CH_4–HF relationship, calculated from the Halogen Occultation Experiment (HALOE) satellite and the JPL MkIV Interferometer data. Wang et al. (2014) similarly use the relationship between stratospheric nitrous oxide (N_2O) and CH_4 and the fact that tropospheric N_2O is well known to infer stratospheric variations in N_2O, and hence CH_4. Angelbratt et al. (2011) remove the Network for the Detection of Atmospheric Composition Change (NDACC) CH_4 total column variability with a multiple regression model that parameterizes anomalies of several measurements, including HF, carbon monoxide, ethane, and tropopause height. Sepúlveda et al. (2012) use the retrieval algorithm PROFFIT to infer vertical CH_4 profiles directly from the absorption line shapes of the mid-infrared (MIR) FTS spectra measured within NDACC, comparing the resulting tropospheric columns with those calculated with a HF proxy method. Extending this study to additional sites, Sepúlveda et al. (2014) estimate a precision of 0.5 % and a systematic error of 2.5 % for daily mean values of tropospheric CH_4 derived from profile retrievals on the MIR NDACC measurements.

Vertical profile retrievals using the TCCON spectra are more difficult than those using NDACC MIR spectra because the NDACC measurements apply spectral filters to narrow the spectral coverage, yielding higher signal-to-noise ratios at higher spectral resolution, at the expense of making simultaneous measurements of some other gases. In addition, the line strengths in the MIR are generally higher and doppler widths are smaller, allowing more degrees of freedom in the vertical retrieval. Nevertheless, profile retrievals are more sensitive to error in the instrument and assumed spectroscopic line shapes than profile-scaling retrievals. Quantifying the variability of stratospheric CH_4 via a chemical tracer is, however, not without challenge, as this method is sensitive to errors in the representation of the relationship between that tracer and CH_4 in the stratosphere and knowledge of their respective averaging kernels. In addition, this method provides no information about vertical structure within the troposphere.

To determine the stratospheric CH_4 component of the FTS-retrieved total column, we propose to use its relationship with HF, which is measured at almost all TCCON sites. Stratospheric CH_4 has a nearly linear inverse relationship with HF, which exists almost exclusively in the stratosphere (Luo et al., 1995; Washenfelder et al., 2003). The photodissociation of chlorofluorocarbons (CFCs) and the resulting carbonyl products produce free fluorine, which can then in turn react with CH_4 and water vapor (H_2O) to produce HF, the most stable reservoir species of fluorine in the stratosphere (Luo et al., 1994). The reactions producing HF occur in the middle-high stratosphere, leading to a uniformly increasing vertical profile (Luo et al., 1995). CH_4, by contrast, is transported from the troposphere and is destroyed by O(1D), hydroxyl, and chlorine free radical-initiated oxidation. The resulting nearly linear relationship between HF and stratospheric CH_4, which is seasonally and zonally consistent, makes HF a useful proxy for the contribution of stratospheric variability to the CH_4 total column.

2 Derivation of tropospheric CH_4 columns

TCCON FTS retrievals are conducted with the GFIT nonlinear least-squares fitting algorithm, which determines a vertical scale factor (γ) of an a priori vertical profile ($\boldsymbol{x}^{\mathrm{a}}$) based on the best spectral fit of the solar absorption signal. The scaled profile is then vertically integrated, and the resulting column abundance is divided by the vertical column of dry air, calculated using the retrieved column of oxygen (O_2) (Wunch et al., 2010, 2011a).

The retrieved integrated column of CH_4 can be expressed as a first order Taylor expansion about the solution $\gamma_{\mathrm{CH_4}} c^{\mathrm{a}}_{\mathrm{CH_4}}$ (Rodgers and Connor, 2003) such that,

$$\hat{c}_{\mathrm{CH_4}} = \gamma_{\mathrm{CH_4}} \cdot c^{\mathrm{a}}_{\mathrm{CH_4}} + \boldsymbol{a}^{\S}_{\mathrm{CH_4}} (\boldsymbol{x}_{\mathrm{CH_4}} - \gamma_{\mathrm{CH_4}} \boldsymbol{x}^{\mathrm{a}}_{\mathrm{CH_4}}), \quad (1)$$

where $\hat{c}$ is the retrieved column, $\gamma_{\mathrm{CH_4}}$ is the retrieved profile scale factor of CH_4, $\boldsymbol{x}$ is the true profile, and $\boldsymbol{x}^{\mathrm{a}}_{\mathrm{CH_4}}$ and $c^{\mathrm{a}}_{\mathrm{CH_4}}$ are the a priori vertical profile and column-integrated CH_4, respectively. We define § as an operator that represents the pressure-weighted integration of the profile:

$$\boldsymbol{a}^{\S}\boldsymbol{x} = \sum_{i=1}^{N} a_i \cdot h_i \cdot x_i, \quad (2)$$

where $\boldsymbol{a}$ is the FTS column averaging kernel, dependent on solar zenith angle and pressure, $\boldsymbol{h}$ is the pressure-weighting function, such that $\hat{c} = \boldsymbol{h}^T \hat{\boldsymbol{x}}$ (Connor et al., 2008; Wunch et al., 2011b), and i is the index of pressure levels from the surface to the highest level, N. When the vertical column includes water vapor, such as in the case of the priors, the

pressure-weighting function incorporates the H_2O profile to convert $\boldsymbol{x}$ to dry-air mole fractions.

To isolate the tropospheric column of CH_4, we assume a linear relationship between CH_4 and HF in the stratosphere such that

$$\boldsymbol{x}_{CH_4} = c^{trop}_{CH_4}\boldsymbol{u} + \beta \boldsymbol{x}_{HF}, \quad (3)$$

where $c^{trop}_{CH_4}$ represents the pressure-weighted DMF averaged over the tropospheric column, $\boldsymbol{u}$ is a unity vector the length of the number of vertical levels in the total column retrieval integration, and β is the time-dependent CH_4–HF slope in the stratosphere. Integrating the vertical profiles, the column-averaged form of this relationship becomes

$$c_{CH_4} = c^{trop}_{CH_4} + \beta c_{HF}, \quad (4)$$

where c is the total column DMF of the respective trace gases. The βc_{HF} term is negative and represents the amount of CH_4 that has been destroyed in the stratosphere, rather than the stratospheric partial column of CH_4. We also assume that the a priori CH_4 profiles can be approximated using the linear relationship between CH_4 and HF.

By combining Eqs. (3) and (4), as well as their analogs for the a priori profiles, into Eq. (1), we derive a tropospheric column-average DMF:

$$c^{trop}_{CH_4} = \hat{c}_{CH_4} - \beta\left(\gamma_{CH_4}\cdot c^{a}_{HF} + \boldsymbol{a}^{\S}_{CH_4}(\boldsymbol{x}_{HF} - \gamma_{CH_4}\boldsymbol{x}^{a}_{HF})\right). \quad (5)$$

Ideally, $\boldsymbol{x}_{\mathbf{HF}}$ would be derived from the equivalent of Eq. (1) for HF, but doing so would require inverting the pressure-weighted averaging kernel, which does not have a unique solution. Thus, in order to solve Eq. (5), we must assume that $\boldsymbol{x}_{HF} = \hat{\boldsymbol{x}}_{HF} = \gamma_{HF}\boldsymbol{x}^{a}_{HF}$ and, accordingly, that the shape of the HF profile is known. In general, this is a reasonable assumption because the vertical profile is governed mainly by well-characterized chemical production, and, as previously stated, increases uniformly. However, this solution has limitations when the scaled profile deviates from the true profile, such as in the polar vortex.

Substituting $\gamma_{HF}\boldsymbol{x}^{a}_{HF}$ for $\boldsymbol{x}_{HF}$, the tropospheric column of CH_4 is derived as follows:

$$c^{trop}_{CH_4} = \hat{c}_{CH_4} - \beta\left(\gamma_{CH_4}\cdot c^{a}_{HF} + \boldsymbol{a}^{\S}_{CH_4}\boldsymbol{x}^{a}_{HF}(\gamma_{HF} - \gamma_{CH_4})\right). \quad (6)$$

All of the terms on the right hand of the equation can be generated from the TCCON data set except for β, which we derive from satellite data. Equation (6) can be applied to determine tropospheric DMFs of trace gases other than CH_4 that are correlated with HF in the stratosphere because it does not require assumptions about the relationship between the averaging kernels of the respective gases and is thus a more general approach than that of Washenfelder et al. (2003).

2.1 Measurement uncertainties

The $c^{trop}_{CH_4}$ error is calculated by propagating the uncertainties of the retrievals, which in Eq. (6) are associated with the vertical scale factors, and β, which is described in Sect. 2.2. These errors are propagated as the sum of the squares of the standard errors for each term. Because the vertical scale factor errors are derived assuming that the residuals from the spectral fits have a Gaussian distribution, systematic artifacts that are stable from spectrum to spectrum inflate the errors calculated from the spectral fit. To derive the measurement precision, the uncertainties are scaled to account for the variations in DMFs calculated from successive spectra within 5 min. The mean and median tropospheric CH_4 precisions vary from 0.04–1 and 0.01–0.03 %, respectively, at individual sites and are 0.1 and 0.004 % across all sites and years. By comparison, the precision in Washenfelder et al. (2003) is 0.5 %, although this improvement is partially attributable to advancements in the retrieval methodology and instrumentation.

The data have been corrected for laser sampling errors (Dohe et al., 2013; Messerschmidt et al., 2010), and the associated uncertainties of those corrections are summed in quadrature with the measurement precision.

2.2 Determination of CH_4–HF slope

Vertical profiles of CH_4 and HF mole fractions were developed from level 2, version 3.0 and 3.5 retrievals from the Atmospheric Chemistry Experiment Fourier Transform Spectrometer (ACE-FTS) instrument on the Canadian SCISAT-1 satellite. SCISAT-1 orbits in low Earth orbit with an inclination of 74°, offering coverage of tropical, mid-latitude and polar regions from 85° N to 85° S (Bernath, 2005; De Mazière et al., 2008; Mahieu et al., 2008; Waymark et al., 2014). Data were taken from February 2004 through September 2010 for version 3.0 and October 2010 through December 2012 for version 3.5. These data sets differ only in that the a priori pressure and temperature profiles in the latter are taken from the global Canadian Meteorological Center model rather than the regional one, which began to provide unphysical profiles starting October 2010 (Waymark et al., 2014). The ACE-FTS profiles are additionally filtered to exclude occultations with physically unlikely profiles and all individual CH_4 and HF retrievals with statistical fitting errors above 5 %. Because the HF abundance in the troposphere is essentially zero, any coincident retrievals of CH_4 and HF were assumed to reside in the stratosphere; therefore we did not designate a pressure level threshold to isolate the stratosphere. Data above 70 km were excluded for consistency with TCCON retrievals, although CH_4 concentrations are generally depleted at that altitude. The CH_4–HF relationship exhibits a strong altitude dependence, with steeper CH_4–HF slopes in the upper stratosphere (Fig. 1). Annual slopes follow the long-term trend from Washenfelder et al. (2003),

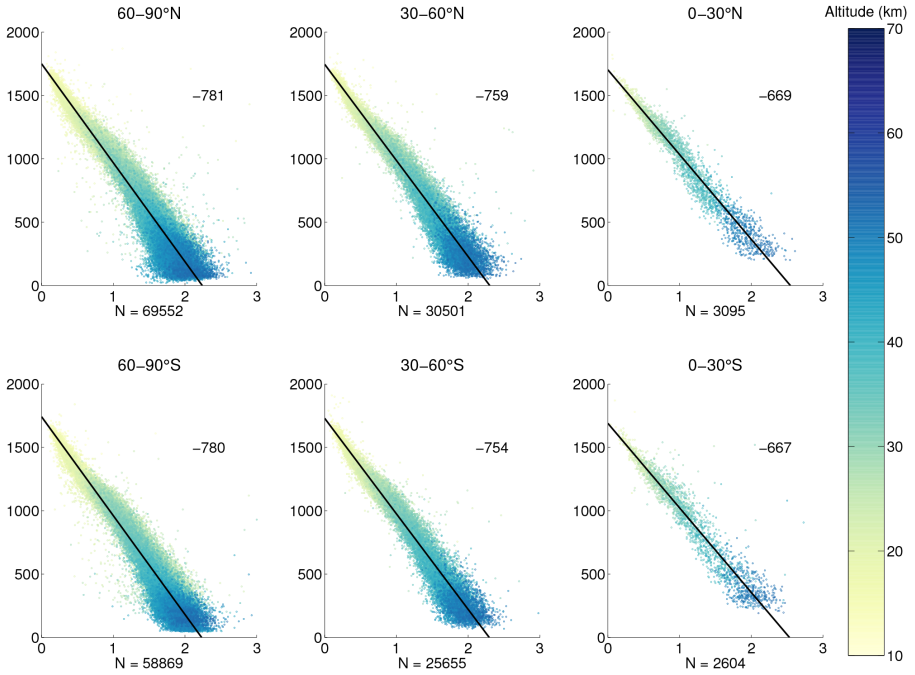

Figure 1. CH_4 (ppb, y axis) vs. HF (ppb, x axis) from ACE-FTS measurements taken between 2004–2012, binned by zonal bands. The slopes of the linear regression are in the upper right-hand corner, and number of data points (N) are listed below each plot.

given the expected trajectory of HF concentrations in the stratosphere (Fig. 2).

Tracer–tracer relationships in the stratosphere tend to be dependent on latitude, with the tropics exhibiting different slopes than the mid-latitude "surf zone" and the polar regions (Luo et al., 1995). While ACE-FTS coverage at high latitudes is extensive, tropical coverage is sparse; thus, to ensure a large enough number of data points in the tropics for robust statistical analysis, we binned CH_4 and HF mole fractions in 30° zonal bands. The tracer relationship demonstrates a clear zonal trend: the slopes are less steep in lower latitudes, and the Northern Hemisphere slopes are more steep than their zonal counterparts in the Southern Hemisphere (Figs. 1, 2). To determine statistically robust values for β, the CH_4–HF slope was computed for bootstrap subsamples of 1000 individual retrievals from each year and zonal band. In order to minimize the effect of outliers in the determination of the slope, we applied an iteratively re-weighted least squares regression with a Tukey's bi-weight function, weighting data points by pressure (Hoaglin et al., 1983). The means and 2σ standard deviations of the resulting probability distributions were taken respectively as the values and errors of β (Table 1). For 2013, we calculated the annual growth rate of the CH_4–HF ratio in the northern mid-latitude region (30–60° N), chosen because the surf zone is well-mixed and thus has the most robust tracer relationships, and added it to the respective zonal values for 2012. The error for β in 2013 was computed as the sum in quadrature of the error for β in 2012, the standard error of the annual growth rate, and the

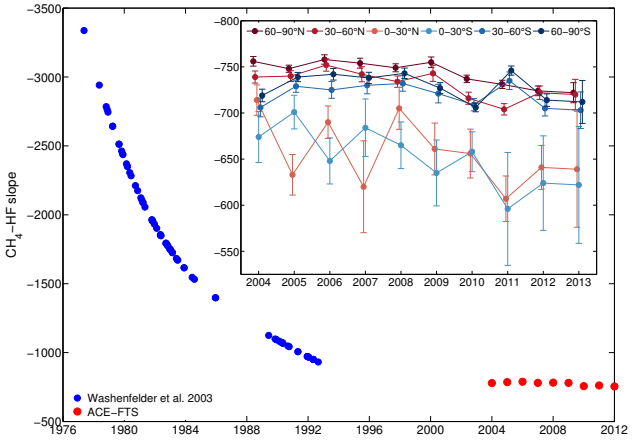

Figure 2. Long-term CH_4–HF slopes derived by Washenfelder et al. (2003) and annual-mean slopes from ACE-FTS measurements. The inset shows the time series of zonal pressure-weighted ACE-FTS slopes (β), with error bars denoting the 2σ standard error. For each year, zonal slopes are offset from each other for clarity.

2σ standard deviations of the interannual variability of each zonal band. While temporal trends in β do indicate seasonal variability, the impact on the slopes is not sufficiently statistically robust from year to year to incorporate a seasonally varying β. The sensitivity of the tropospheric methane calculation to β differs by site, but generally varies by 0.1–1 ppb for $\Delta\beta$ of 10.

Table 1. Annual zonal values (2σ uncertainties) of β.

	60–90° S	30–60° S	0–30° S	0–30° N	30–60° N	60–90° N
2004	−719 (7)	−706 (10)	−674 (28)	−714 (17)	−739 (7)	−756 (5)
2005	−739 (5)	−729 (7)	−701 (18)	−633 (22)	−740 (6)	−748 (4)
2006	−742 (6)	−725 (9)	−648 (25)	−690 (18)	−752 (7)	−758 (5)
2007	−738 (6)	−730 (9)	−684 (31)	−620 (50)	−742 (8)	−754 (5)
2008	−743 (6)	−732 (8)	−665 (25)	−705 (23)	−734 (6)	−749 (4)
2009	−727 (6)	−721 (10)	−635 (36)	−661 (28)	−743 (9)	−755 (6)
2010	−706 (5)	−709 (7)	−658 (22)	−656 (27)	−716 (7)	−737 (4)
2011	−746 (5)	−735 (9)	−596 (61)	−607 (25)	−704 (6)	−731 (4)
2012	−714 (7)	−705 (8)	−624 (51)	−641 (24)	−722 (7)	−724 (5)
2013	−712 (23)	−703 (20)	−622 (63)	−639 (63)	−720 (16)	−722 (11)

2.3 Validation of methodology

Equation (6) incorporates two major assumptions: that the CH_4–HF relationship is linear, and that the retrieved HF column is a close approximation to the true HF column. To test these assumptions, we compared tropospheric CH_4 DMFs derived directly from ACE-FTS CH_4 profiles to those calculated by substituting the most recent TCCON priors (GGG 2014) and ACE-FTS CH_4 and HF profiles into Eq. (5). For this analysis, the ACE-FTS trace gas profiles up to 70 km interpolated onto a 1 km vertical grid were considered the true profiles $\boldsymbol{x}_{\mathrm{HF}}$ and $\boldsymbol{x}_{\mathrm{CH_4}}$, and assuming $\gamma_{\mathrm{CH_4}} \approx 1$, we solved Eqs. (1) and (5) for $c^{\mathrm{trop}}_{\mathrm{CH_4}}$. Because the minimum retrieval altitudes were at least 5.5 km and on average 9.5 km, mole fractions of CH_4 and H_2O near the surface were extrapolated using TCCON priors. Occultations with individual CH_4, HF and H_2O errors greater than 10 % were excluded for latitudes poleward of $\pm 30°$. In the tropics, the error threshold was relaxed to 40 % in order to ensure a large enough data set for results to be meaningful. We then compared the calculated tropospheric methane column-averaged DMF to the ACE-FTS CH_4 profiles integrated to the tropopause. For the intercomparison, the integrated ACE-FTS profiles were smoothed with the TCCON CH_4 averaging kernel and priors (Connor et al., 2008; Wunch et al., 2011b). The tropopause altitude was calculated using National Centers for Environmental Prediction/National Center for Atmospheric Research (NCEP/NCAR) Reanalysis local noon temperature profiles(Kalnay et al., 1996), from which the TCCON priors are generated, for consistency.

As Fig. 3 illustrates, the temporal and zonal dependencies of the tropospheric methane calculation are well characterized, with a few notable exceptions. The consistency of the bias across years (slope = 0.99–1) indicates that the annual variability of β is accurate, although the asymmetric scatter of the residuals in the northern tropics could be a result of the smaller number of data points included in the determination of β. Additionally, the seasonal variability associated with descent within the polar vortices, not currently captured by the HF priors, accounts for the outliers apparent in higher latitudes. Because the southern polar vortex is stronger and more persistent than in the north, the calculated tropospheric column exhibits a much larger spread in the southern polar zonal band.

The underestimation of tropospheric CH_4 in the Northern Hemisphere and slight overestimation in the Southern Hemisphere is partially a result of several assumptions that are necessary because coincident TCCON measurements do not exist for all zonal regions over the time series. TCCON averaging kernels are highly dependent on the solar zenith angle and surface pressure at the time of measurement; however, the solar zenith angles at the surface during ACE-FTS occultations are close to 90°, and the surface pressure is unknown. To address the latter, we assume that the pressure at the lowest point in the ACE-FTS profile is the surface pressure. We also use the solar zenith angle calculated at the latitude, longitude and time of the occultation, which, while accurate, does not test one of the main advantages of this methodology, which is to adjust the tropospheric CH_4 calculation for seasonality and latitude, which impacts each zonal band differently and thus creates an offset.

The method validation also requires the assumption that $\gamma_{\mathrm{CH_4}} = 1$ in Eqs. (1) and (5). A bias in the a priori profiles between the Northern and Southern Hemispheres would lead to differences in the retrieved values of $\gamma_{\mathrm{CH_4}}$, indicating that the TCCON a priori profiles are slightly too low in the Southern Hemisphere relative to the Northern Hemisphere. While $\gamma_{\mathrm{CH_4}}$ is generally within 1 % of 1, TCCON measurements tend to have larger values for $\gamma_{\mathrm{CH_4}}$ in the Southern Hemisphere compared to the Northern Hemisphere, and a difference of 0.01 between hemispheres can shift the residuals from the one-to-one line by up to 4 ppb, or about one quarter of the offset in the mid-latitudes. Because of the low sensitivity of the tropospheric CH_4 calculation to changes in β, inter-hemispheric biases in β determined from ACE-FTS would have to be considerable to explain the offset.

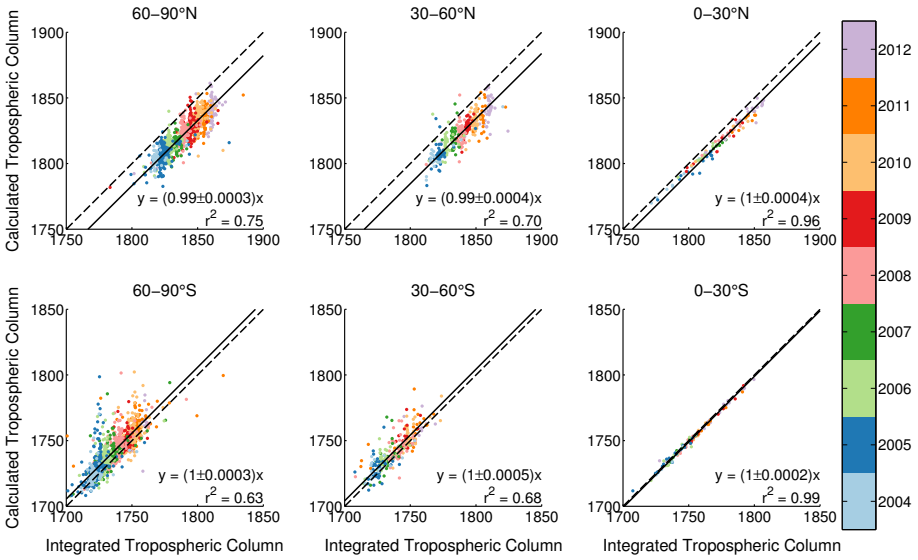

Figure 3. Validation of the tropospheric column-averaged CH_4 derivation using HF as a proxy. The calculated tropospheric CH_4 (y axis) uses the TCCON priors, CH_4 averaging kernel and ACE-FTS vertical profiles to determine the value that the ground-based FTS would retrieve. The integrated tropospheric CH_4 (x axis) applies the pressure-weighting function and TCCON CH_4 averaging kernel and priors to the extrapolated tropospheric ACE-FTS profile of CH_4. The black lines depict the one-to-one line (solid) and the linear regression of the calculated vs. integrated tropospheric CH_4 with a zeroed y intercept (dashed). The r^2 values correspond to the linear regression. Note the different DMF ranges in the Northern vs. Southern Hemispheres.

Table 2. TCCON sites, coordinates, altitudes, and locations used in this analysis.

Site	Latitude	Longitude	Elevation (km)	Location
Sodankylä	67.4	26.6	0.18	Sodankylä, Finland
Bremen	53.1	8.85	0.03	Bremen, Germany
Park Falls	45.9	−90.3	0.44	Park Falls, WI
Lamont	36.6	−97.5	0.32	Lamont, OK
Izaña	28.3	−16.5	2.37	Tenerife, Canary Islands
Darwin	−12.4	130.9	0.03	Darwin, Australia
Wollongong	−34.4	150.9	0.03	Wollongong, Australia
Lauder	−45.0	169.7	0.37	Lauder, NZ

3 Results

Tropospheric column-averaged DMFs were calculated for TCCON sites in Sodankylä (Fig. 4a), Bremen (Fig. 4b), Park Falls (Fig. 4c), Lamont (Fig. 4d), Izaña (Fig. 4e), Darwin (Fig. 4f), Wollongong (Fig. 4g) and Lauder (Fig. 4h) using the 2012 version of the GGG software. Location information for each of these TCCON sites can be found in Table 2. As we would expect, the tropospheric column-averaged DMFs of CH_4 are higher than the total column DMFs. Many of the low outliers in the total column that are a result of the stratospheric variability no longer appear in the tropospheric DMFs. The intraday variability of the tropospheric DMFs are generally equivalent to those of the corresponding total column DMFs, although the tropospheric standard deviations are, in some cases, significantly larger than those of the total column. Sites in the tropics are especially susceptible to both larger errors for a single measurement and larger daily variances due to the higher HF errors caused by H_2O interference (e.g., Darwin, Fig. 4f). Additionally, the tropospheric calculation removes most of the effects of the seasonal cycle of stratospheric variability. While the magnitude of the impact on the seasonal cycle of CH_4 varies from site to site, the tropospheric column calculation generally shifts the peak of CH_4 from late fall to winter and the minimum from spring to late summer (Fig. 5). At Lamont and Park Falls, this impact is especially apparent, with 2-month lags in the maxima and minima in the tropospheric versus total columns. The detrended seasonal cycles of the tropospheric CH_4 also exhibit fewer short-term fluctuations, except in the case of Izaña, which is located on a mountain at about 2.4 km and thus is more sensitive to the free troposphere.

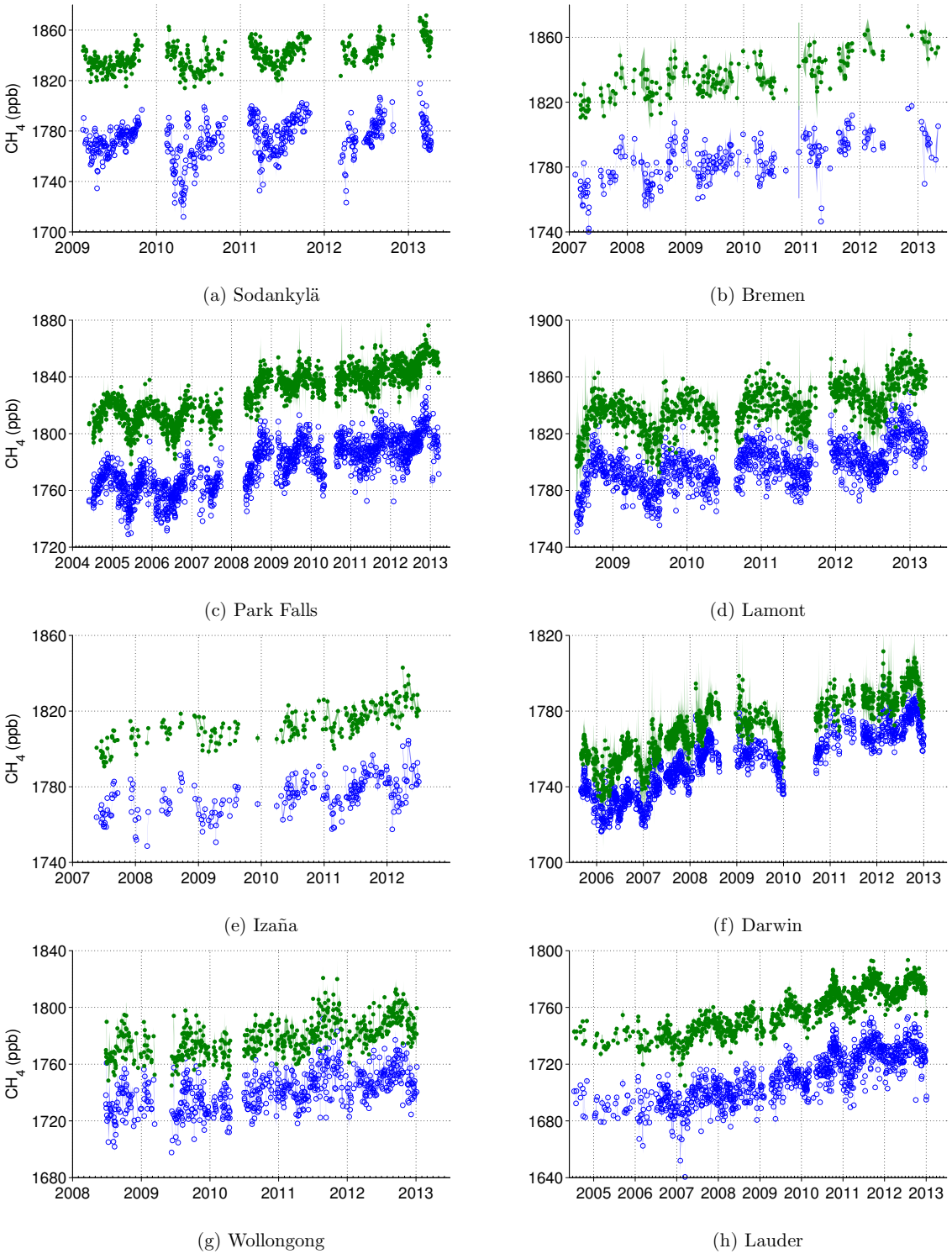

Figure 4. Daily median and standard deviation (shading) total (blue, open circles) and tropospheric (green, closed circles) column-averaged DMFs of CH_4 at **(a)** Sodankylä, Finland, **(b)** Bremen, Germany, **(c)** Park Falls, Wisconsin, USA, **(d)** Lamont, Oklahoma, USA, **(e)** Izaña, Tenerife, Canary Islands, **(f)** Darwin, Australia, **(g)** Wollongong, Australia and **(h)** Lauder, New Zealand. Only days with more than 10 measurements of tropospheric CH_4 with errors of $< 1\,\%$ are shown. Both the 120 HR (June 2004–December 2010) and 125 HR (February 2010–December 2012) instruments are plotted for Lauder.

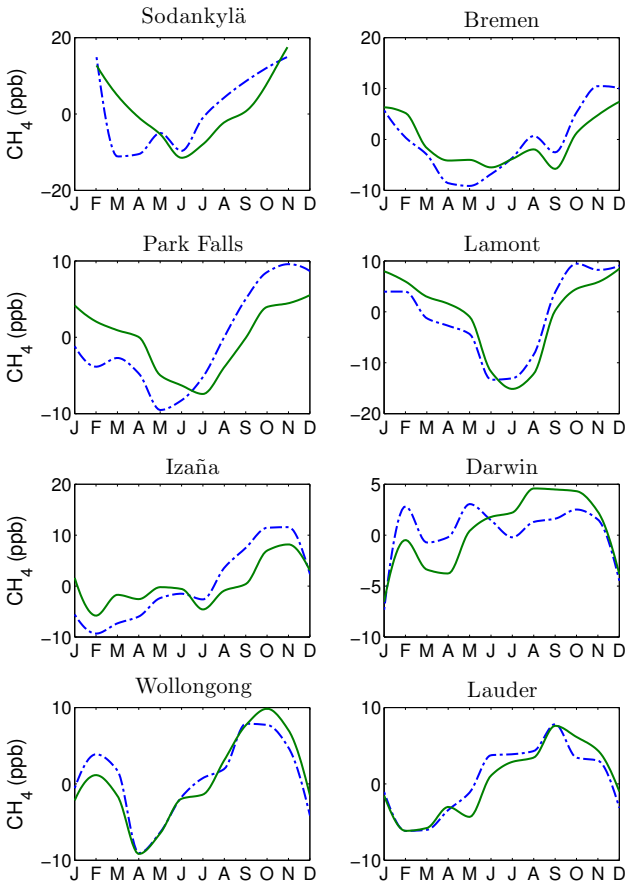

Figure 5. De-trended seasonal cycles of CH_4 for total (blue, dashed) and tropospheric (green, solid) columns averaged over all years.

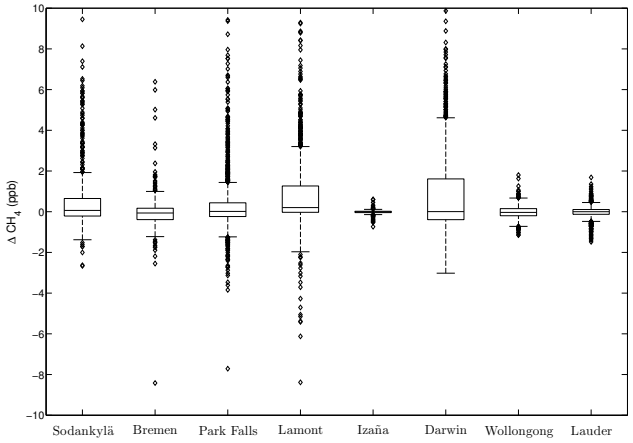

Figure 6. The differences between daily tropospheric CH_4 standard deviations using the Washenfelder et al. (2003) and updated methods. (Positive values correspond to larger Washenfelder et al. (2003) standard deviations.) Box ends, midline and whiskers illustrate the quartiles, medians and twice the interquartile ranges, respectively. Outliers beyond the the range are denoted by diamonds.

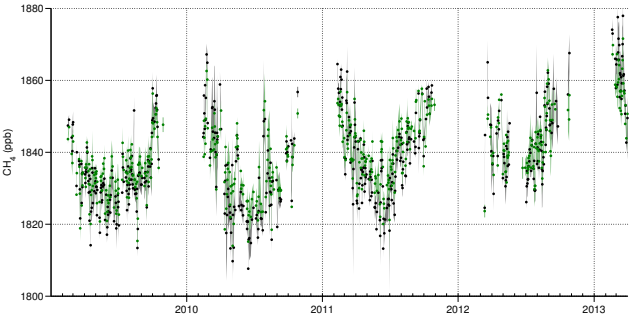

Figure 7. Daily median tropospheric column-averaged DMFs at Sodankylä using the Washenfelder et al. (2003) method (black) vs. the updated method (green). Tropospheric column DMFs are the same as in Fig. 4.

3.1 Comparison to Washenfelder method

The derivation introduced here improves on the previous calculation of Washenfelder et al. (2003) by explicitly including the CH_4 averaging kernels in the estimate of stratospheric loss and including the recent ACE-FTS satellite data set, which allows for the analysis of temporal and zonal dependencies. To assess the impacts of these additions to the tropospheric CH_4 column, we calculated the tropospheric CH_4 DMFs using the Washenfelder et al. (2003) derivation (Eq. 4) and the annual northern mid-latitude values of β (Table 1, column 6) for all sites. The daily standard deviations tend to decrease modestly with the updated methodology (Fig. 6), although intraday variability is reduced by up to 40 ppb. The inclusion of the CH_4 averaging kernel adjusts the air-mass dependence of the tropospheric CH_4 calculation, thereby reducing the amplitude of the CH_4 seasonal cycle. This improvement is especially apparent during winter at the high-latitude sites (Fig. 7), because the solar zenith angles are large and, therefore, the CH_4 averaging kernels have a strong dependence on altitude. Additionally, calculating the CH_4–HF relationship as a function of latitude allows for more meaningful geospatial comparisons.

3.2 Comparison to in situ measurements

Following the method for numerical integration of in situ profiles derived in Wunch et al. (2010), smoothed column-averaged DMFs determined for from several aircraft campaigns (Table 3). Additional information on the TCCON calibration, including instruments, can be found in Wunch et al. (2010), and the WMO calibration scales used for the instruments can be found in Dlugokencky (2005). Aircraft profiles were integrated to the tropopause, determined using the flight temperature profiles. Aircraft errors are calculated as the sum in quadrature of the respective 2σ instrument errors and the estimated uncertainties associated with the profile not reaching the tropopause and the surface. FTS columns were calculated with the aircraft calibration factors for CH_4 determined

Table 3. Aircraft Overflights. TCCON site locations and aircraft campaign dates and altitude ranges are listed.

Site	Location	Campaign	Date	Altitude Range
Bremen	53° N, 9° E	IMECC	9 Oct 2009	0.5–13.2 km
Park Falls	46° N, 90° W	INTEX	12 Jul 2004	0.7–10.1 km
		START08	12 May 2008	1.2–9.4 km
Lamont	37° N, 98° W	HIPPO	30 Jan 2009	0.4–13.0 km
		Learjet	31 Jul; 2, 3 Aug 2009	0.5–12.9 km
Wollongong	34° S, 151° E	HIPPO	15 Nov 2009	0.1–12.6 km
Lauder	45° S, 170° E	HIPPO	20 Jan 2009	0.7–14.6 km

in Wunch et al. (2010) applied to the tropospheric column and thus do not include the spectroscopy bias that exists in the total column. FTS errors are calculated as the standard deviation of tropospheric DMFs with individual errors of less than 1 % measured within 1 hour of each flight. Both the slope and associated error are calculated considering both the aircraft and FTS errors, assuming those errors are independent of each other, following the method outlined in York et al. (2004). Additionally, because the derivation method is predicted to vary linearly, we calculate the slope assuming a y intercept of zero.

The FTS tropospheric columns show general agreement to each other (Fig. 8), with a slope close to within error of the one-to-one line and a slope and error similar to that of total column CH_4 (Wunch et al., 2010). The tropospheric column calibration curve has a slight hemispheric bias, with Southern Hemisphere sites above the fit line and Northern Hemisphere sites below, with the INTEX-NA campaign, over Park Falls, WI, as the only exception.

Additionally, we compared the tropospheric CH_4 to long-term in situ flask measurements collected at the Atmospheric Radiation Measurement Program (ARM), Southern Great Plains (SGP) site, near the Lamont TCCON station, and analyzed by the NOAA Earth System Research Laboratory (ESRL). Surface measurements are collected from a 60 m tower, typically once per week on one afternoon, and aircraft samples are collected approximately biweekly with a flight path centered over the tower. The integrated aircraft DMFs are generally higher than the TCCON tropospheric columns, which provide a lower bound to the flask measurements (Fig. 9a). The partial aircraft columns, restricted to the free troposphere (approximately 3–7 km), are more consistent with the TCCON tropospheric columns. The calibration curve reinforces the distinction between the aircraft tropospheric and partial tropospheric columns when compared to the FTS DMFs at Lamont (Fig. 9b); while the best fit slopes, calculated as in (Fig. 8), are equal within measurement error, the slope of the free troposphere partial column has a smaller offset from the FTS-aircraft one-to-one line.

In situ measurements at the surface are also useful for regions without large local surface sources and if the troposphere is well-mixed, as in New Zealand. We compared Lauder FTS measurements to in situ data at the Baring Head

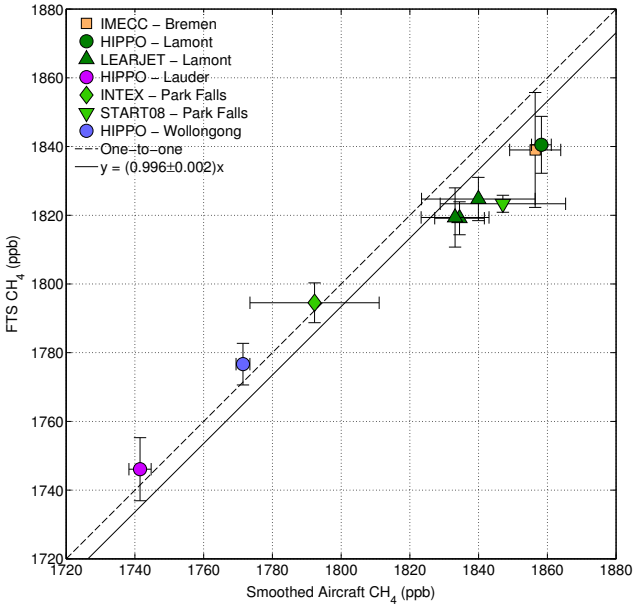

Figure 8. Tropospheric CH_4 column comparison for TCCON vs. aircraft profiles. Error bars denote the 2σ standard deviation from the daily median (FTS) and the estimated instrument errors and tropospheric uncertainty of the measurements (aircraft).

National Institute of Water and Atmospheric Research of New Zealand (NIWA) facility, about 600 km northeast of the TCCON site (41.4° S, 174.9° E, 85 m a.s.l.). The Baring Head flask measurements are collected on a stationary platform at a sampling height of 10 m, analyzed with a flame ionizing detector, and calibrated with the NOAA04 scale (Lowe et al., 1991). The surface measurements are similar to the tropospheric columns, both in terms of the DMF values and the timing of the seasonal cycle (Fig. 10). The Lauder tropospheric columns are somewhat higher in the late summer and early fall, which could be a function of local CH_4 sources near Lauder, changing wind directions impacting the covariance between the two sites, or seasonal HF variability not captured in the tropospheric column derivation. Given the relatively large discrepancy of about 10 ppb between the two data sets during those months and the low sensitivity of the tropospheric column to small changes in β, the last of these explanations is the least likely.

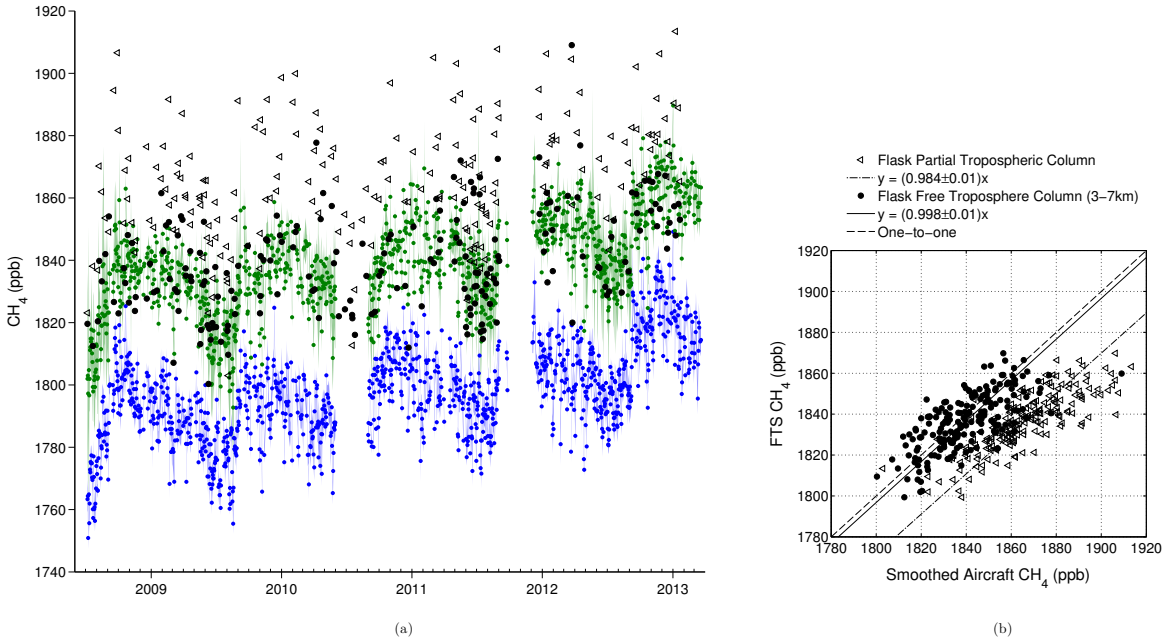

Figure 9. (a) Daily median column and aircraft CH_4 DMFs at Lamont. Flask partial tropospheric columns integrate CH_4 from the minimum to the maximum altitudes of the aircraft measurement. Flask free troposphere columns integrate CH_4 from the minimum to the maximum altitudes of the aircraft within 3–7 km. Total and tropospheric column DMFs are the same as in Fig. 4. **(b)** Tropospheric CH_4 column comparison for TCCON vs. in situ profiles.

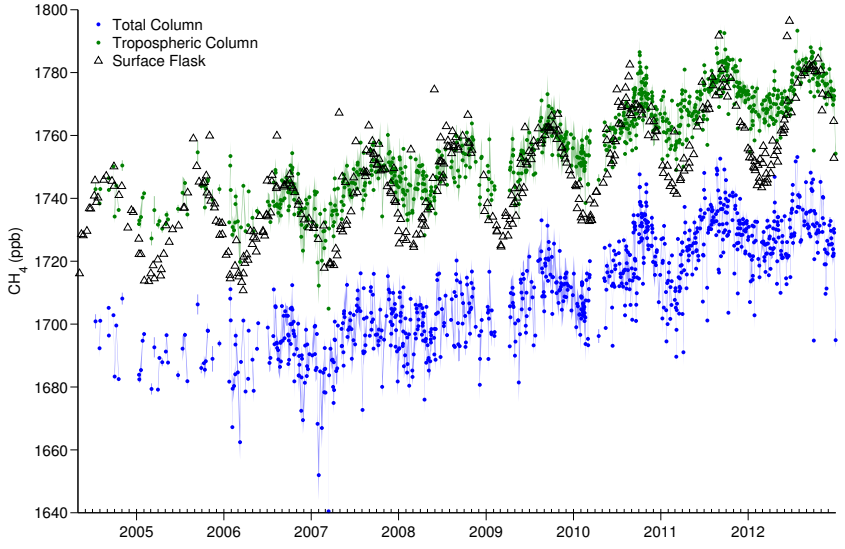

Figure 10. Daily median CH_4 DMFs at Lauder (FTS) and Baring Head (flask). Both the 120 HR (June 2004–December 2010) and 125 HR (February 2010–December 2012) instruments are plotted for Lauder. Total and tropospheric column DMFs are the same as in Fig. 4.

4 Conclusions

Inadequate constraints on the global CH_4 budget have been a long-standing problem, and understanding recent trends depends on reliable and frequent observations of tropospheric CH_4 concentrations. By explicitly taking into account the averaging kernels of CH_4 and incorporating temporally and spatially varying estimates of the CH_4–HF relationship, the methodology described here refines earlier tracer proxy methods for estimating stratospheric CH_4. The tropospheric column measurements of CH_4 derived from TCCON total column-averaged DMFs provide a useful addition to existing data sets used to analyze the global methane cycle and verify chemical transport models.

While the CH_4–HF relationship is robust, the calculation of β still has limitations. The slight non-linearity and seasonal variability of the CH_4–HF relationship could impact the estimation of stratospheric CH_4 loss. Further analysis of ACE-FTS and other high-frequency stratospheric measurements could produce a statistically significant seasonal cycle to apply to β.

Acknowledgements. Support for this research was received from NASA's Carbon Cycle Science program (NNX10AT83G, James Randerson, PI). Part of this work was performed at the Jet Propulsion Laboratory, California Institute of Technology, under contract with NASA. US funding for TCCON comes from NASA grants NNX11AG01G, NAG5-12247, NNG05-GD07G, and NASA Orbiting Carbon Observatory Program. We are grateful to the DOE ARM program for technical support in Lamont and Darwin and Jeff Ayers for technical support in Park Falls. European funding is from GEOMON, InGOS, and IMECC. From 2004 to 2011 the Lauder TCCON program was funded by the New Zealand Foundation of Research Science and Technology contracts CO1X0204, CO1X0703 and CO1X0406. Since 2011 the program has been funded by NIWA's Atmosphere Research Programme 3 (2011/13 Statement of Corporate Intent). Australian funding is from the Australian Research Council, DP0879468 and LP0562346. Funding for the ACE-FTS mission is primarily provided by the Canadian Space Agency. NCEP Reanalysis data are provided by NOAA/OAR/ESRL PSD. SGP aircraft flask data were obtained through the ARM Program sponsored by the US Department of Energy, Office of Science, Office of Biological and Environmental Research and were generated by NOAA-ESRL, Carbon Cycle Greenhouse Gases Group. Baring Head NIWA surface data were provided courtesy of Gordon Brailsford, Dave Lowe and Ross Martin. We would also acknowledge the contributions of in situ vertical profiles from the HIPPO, IMECC, INTEX, Learjet, and START08 campaigns. Color schemes for Figs. 1 and 3 are from Brewer, Cynthia A., 200x. http://www.ColorBrewer.org.

Edited by: G. Stiller

References

Angelbratt, J., Mellqvist, J., Blumenstock, T., Borsdorff, T., Brohede, S., Duchatelet, P., Forster, F., Hase, F., Mahieu, E., Murtagh, D., Petersen, A. K., Schneider, M., Sussmann, R., and Urban, J.: A new method to detect long term trends of methane (CH_4) and nitrous oxide (N_2O) total columns measured within the NDACC ground-based high resolution solar FTIR network, Atmos. Chem. Phys., 11, 6167–6183, doi:10.5194/acp-11-6167-2011, 2011.

Bernath, P. F.: Atmospheric Chemistry Experiment (ACE): mission overview, Geophys. Res. Lett., 32, L15S01, doi:10.1029/2005GL022386, 2005.

Connor, B. J., Boesch, H., Toon, G., Sen, B., Miller, C., and Crisp, D.: Orbiting carbon observatory: inverse method and prospective error analysis, J. Geophys. Res., 113, 1–14, doi:10.1029/2006JD008336, 2008.

De Mazière, M., Vigouroux, C., Bernath, P. F., Baron, P., Blumenstock, T., Boone, C., Brogniez, C., Catoire, V., Coffey, M., Duchatelet, P., Griffith, D., Hannigan, J., Kasai, Y., Kramer, I., Jones, N., Mahieu, E., Manney, G. L., Piccolo, C., Randall, C., Robert, C., Senten, C., Strong, K., Taylor, J., Tétard, C., Walker, K. A., and Wood, S.: Validation of ACE-FTS v2.2 methane profiles from the upper troposphere to the lower mesosphere, Atmos. Chem. Phys., 8, 2421–2435, doi:10.5194/acp-8-2421-2008, 2008.

Dlugokencky, E. J.: Conversion of NOAA atmospheric dry air CH_4 mole fractions to a gravimetrically prepared standard scale, J. Geophys. Res., 110, D18306, doi:10.1029/2005JD006035, 2005.

Dohe, S., Sherlock, V., Hase, F., Gisi, M., Robinson, J., Sepúlveda, E., Schneider, M., and Blumenstock, T.: A method to correct sampling ghosts in historic near-infrared Fourier transform spectrometer (FTS) measurements, Atmos. Meas. Tech., 6, 1981–1992, doi:10.5194/amt-6-1981-2013, 2013.

Hoaglin, D. C., Mosteller, F., and Tukey, J. W.: Understanding robust and exploratory data analysis, 3, Wiley New York, 1983.

Kalnay, E., Kanamitsu, M., Kistler, R., Collins, W., Deaven, D., Gandin, L., Iredell, M., Saha, S., White, G., Woollen, J., Zhu, Y., Leetmaa, A., Reynolds, R., Chelliah, M., Ebisuzaki, W., Higgins, W., Janowiak, J., Mo, K. C., Ropelewski, C., Wang, J., Jenne, R., and Joseph, D.: The NCEP/NCAR 40-year reanalysis project, B. Am. Meteorol. Soc., 77, 437–470, 1996.

Keppel-Aleks, G., Wennberg, P. O., and Schneider, T.: Sources of variations in total column carbon dioxide, Atmos. Chem. Phys., 11, 3581–3593, doi:10.5194/acp-11-3581-2011, 2011.

Lowe, D. C., Brenninkmeijer, C. A. M., Tyler, S. C., and Dlugkencky, E. J.: Determination of the isotopic composition of atmospheric methane and its application in the Antarctic, J. Geophys. Res., 96, 15455, doi:10.1029/91JD01119, 1991.

Luo, M., Cicerone, R. J., Russell III, J. M., and Huang, T. Y. W.: Observations of stratospheric hydrogen fluoride by halogen occultation experiment (HALOE), J. Geophys. Res., 99, 16691–16705, 1994.

Luo, M., Cicerone, R. J., and Russell III, J. M.: Analysis of halogen occultation experiment HF versus CH_4 correlation plots: chemistry and transport implications, J. Geophys. Res., 100, 13927–13937, 1995.

Mahieu, E., Duchatelet, P., Demoulin, P., Walker, K. A., Dupuy, E., Froidevaux, L., Randall, C., Catoire, V., Strong, K., Boone, C. D., Bernath, P. F., Blavier, J.-F., Blumenstock, T., Coffey, M., De Mazière, M., Griffith, D., Hannigan, J., Hase, F., Jones, N., Jucks, K. W., Kagawa, A., Kasai, Y., Mebarki, Y., Mikuteit, S., Nassar, R., Notholt, J., Rinsland, C. P., Robert, C., Schrems, O., Senten, C., Smale, D., Taylor, J., Tétard, C., Toon, G. C., Warneke, T., Wood, S. W., Zander, R., and Servais, C.: Validation of ACE-FTS v2.2 measurements of HCl, HF, CCl3F and CCl2F2 using space-, balloon- and ground-based instrument observations, Atmos. Chem. Phys., 8, 6199–6221, doi:10.5194/acp-8-6199-2008, 2008.

Messerschmidt, J., Macatangay, R., Notholt, J., Petri, C., Warneke, T., and Weinzierl, C.: Side by side measurements of CO_2 by ground-based Fourier transform spectrometry (FTS), Tellus B, 62, 749, doi:10.1111/j.1600-0889.2010.00491.x, 2010.

Payne, V. H., Clough, S. A., Shephard, M. W., Nassar, R., and Logan, J. A.: Information-centered representation of retrievals with limited degrees of freedom for signal: application to methane

from the tropospheric emission spectrometer, J. Geophys. Res., 114, D10307, doi:10.1029/2008JD010155, 2009.

Rodgers, C. D. and Connor, B. J.: Intercomparison of remote sounding instruments, J. Geophys. Res., 108, 4116, doi:10.1029/2002JD002299, 2003.

Sepúlveda, E., Schneider, M., Hase, F., García, O. E., Gomez-Pelaez, A., Dohe, S., Blumenstock, T., and Guerra, J. C.: Long-term validation of tropospheric column-averaged CH_4 mole fractions obtained by mid-infrared ground-based FTIR spectrometry, Atmos. Meas. Tech., 5, 1425–1441, doi:10.5194/amt-5-1425-2012, 2012.

Sepúlveda, E., Schneider, M., Hase, F., Barthlott, S., Dubravica, D., García, O. E., Gomez-Pelaez, A., González, Y., Guerra, J. C., Gisi, M., Kohlhepp, R., Dohe, S., Blumenstock, T., Strong, K., Weaver, D., Palm, M., Sadeghi, A., Deutscher, N. M., Warneke, T., Notholt, J., Jones, N., Griffith, D. W. T., Smale, D., Brailsford, G. W., Robinson, J., Meinhardt, F., Steinbacher, M., Aalto, T., and Worthy, D.: Tropospheric CH_4 signals as observed by NDACC FTIR at globally distributed sites and comparison to GAW surface in situ measurements, Atmos. Meas. Tech., 7, 2337–2360, doi:10.5194/amt-7-2337-2014, 2014.

Wang, Z., Deutscher, N. M., Warneke, T., Notholt, J., Dils, B., Griffith, D. W. T., Schmidt, M., Ramonet, M., and Gerbig, C.: Retrieval of tropospheric column-averaged CH_4 mole fraction by solar absorption FTIR-spectrometry using N_2O as a proxy, Atmos. Meas. Tech. Discuss., 7, 1457–1493, doi:10.5194/amtd-7-1457-2014, 2014.

Washenfelder, R. A., Wennberg, P. O., and Toon, G. C.: Tropospheric methane retrieved from ground-based near-IR solar absorption spectra, Geophys. Res. Lett., 30, 2226, doi:10.1029/2003GL017969, 2003.

Waymark, C., Walker, K., Boone, C., and Bernath, P.: ACE-FTS version 3.0 data set: validation and data processing update, Annals of Geophysics, 56, 6339, doi:10.4401/ag-6339, 2014.

Wunch, D., Toon, G. C., Wennberg, P. O., Wofsy, S. C., Stephens, B. B., Fischer, M. L., Uchino, O., Abshire, J. B., Bernath, P., Biraud, S. C., Blavier, J.-F. L., Boone, C., Bowman, K. P., Browell, E. V., Campos, T., Connor, B. J., Daube, B. C., Deutscher, N. M., Diao, M., Elkins, J. W., Gerbig, C., Gottlieb, E., Griffith, D. W. T., Hurst, D. F., Jiménez, R., Keppel-Aleks, G., Kort, E. A., Macatangay, R., Machida, T., Matsueda, H., Moore, F., Morino, I., Park, S., Robinson, J., Roehl, C. M., Sawa, Y., Sherlock, V., Sweeney, C., Tanaka, T., and Zondlo, M. A.: Calibration of the Total Carbon Column Observing Network using aircraft profile data, Atmos. Meas. Tech., 3, 1351–1362, doi:10.5194/amt-3-1351-2010, 2010.

Wunch, D., Toon, G. C., Blavier, J.-F. L., Washenfelder, R. A., Notholt, J., Connor, B. J., Griffith, D. W. T., Sherlock, V., and Wennberg, P. O.: The Total Carbon Column Observing Network, Philos. T. Roy. Soc. A, 369, 2087–2112, doi:10.1098/rsta.2010.0240, 2011a.

Wunch, D., Wennberg, P. O., Toon, G. C., Connor, B. J., Fisher, B., Osterman, G. B., Frankenberg, C., Mandrake, L., O'Dell, C., Ahonen, P., Biraud, S. C., Castano, R., Cressie, N., Crisp, D., Deutscher, N. M., Eldering, A., Fisher, M. L., Griffith, D. W. T., Gunson, M., Heikkinen, P., Keppel-Aleks, G., Kyrö, E., Lindenmaier, R., Macatangay, R., Mendonca, J., Messerschmidt, J., Miller, C. E., Morino, I., Notholt, J., Oyafuso, F. A., Rettinger, M., Robinson, J., Roehl, C. M., Salawitch, R. J., Sherlock, V., Strong, K., Sussmann, R., Tanaka, T., Thompson, D. R., Uchino, O., Warneke, T., and Wofsy, S. C.: A method for evaluating bias in global measurements of CO_2 total columns from space, Atmos. Chem. Phys., 11, 12317–12337, doi:10.5194/acp-11-12317-2011, 2011b.

Yang, Z., Washenfelder, R. A., Keppel-Aleks, G., Krakauer, N. Y., Randerson, J. T., Tans, P. P., Sweeney, C., and Wennberg, P. O.: New constraints on Northern Hemisphere growing season net flux, Geophys. Res. Lett., 34, L12807, doi:10.1029/2007GL029742, 2007.

York, D., Evensen, N. M., Martínez, M. L., and De Basabe Delgado, J.: Unified equations for the slope, intercept, and standard errors of the best straight line, Am. J. Phys., 72, 367, doi:10.1119/1.1632486, 2004.